MOLECULAR ONCOLOGY 6 (2012) 392–404

available at www.sciencedirect.com

SciVerse ScienceDirect

www.elsevier.com/locate/molonc

Co-administration phenoxodiol with doxorubicin synergistically inhibit the activity of sphingosine kinase-1 (SphK1), a potential oncogene of osteosarcoma, to suppress osteosarcoma cell growth both *in vivo* and *in vitro*

Chen Yao[a], *Sujia Wu*[b], *Dong Li*[a], *Huimin Ding*[a], *Zuyu Wang*[a], *Yongjiang Yang*[a], *Shichang Yan*[a], *Zhangping Gu*[a,*]

[a]*Department of Orthopedics, BenQ Medical Center, Nanjing Medical University, Nanjing, Jiangsu 210019, China*
[b]*Department of Orthopedics, Nanjing General Hospital of People's Liberation Army, Nanjing, Jiangsu, China*

ARTICLE INFO

Article history:
Received 21 January 2012
Received in revised form
23 April 2012
Accepted 27 April 2012
Available online 5 May 2012

Keywords:
Sphingosine kinase-1
Osteosarcoma
Doxorubicin
Phenoxodiol
Chemotherapy
Signal transduction

ABSTRACT

Elucidation of the mechanisms of chemo-resistance and implementation of strategies to overcome it will be pivotal to improve the survival for osteosarcoma (OS) patients. We here suggest that sphingosine kinase-1 (SphK1) might be the key factor contributing to chemo-resistance in OS. Our Western-blots and immunohistochemistry results showed that SphK1 is over-expressed in multiple clinical OS tissues. Over-expression of SphK1 in OS cell line U2OS promoted its growth and endorsed its resistance against doxorubicin, while knocking-down of SphK1 by shRNA inhibited U2OS cell growth and increased its sensitivity to doxorubicin. Co-administration phenoxodiol with doxorubicin synergistically inhibited SphK1 activity to trigger cellular ceramide accumulation, and achieved synergistic anti-OS growth effect, accompanied with a significant increased of apoptosis and cytotoxicity. Increased cellular level of ceramide by the co-administration induced the association between Akt and Protein Phosphatase 1 (PP1) to dephosphorylate Akt, and to introduce a constitutively active Akt (CA-Akt) restored Akt activation and diminished cell growth inhibition. Further, phenoxodiol and doxorubicin synergistically activated apoptosis signal-regulating kinase 1(ASK1)/c-jun-NH2-kinase (JNK) signaling, which also contributed to cell growth inhibition. Significantly, the role of SphK1 in OS cell growth and the synergistic anti-OS effect of phenoxodiol and doxorubicin were also seen in a mice OS xenograft model. In conclusion, our data suggest that SphK1 might be a critical oncogene of OS and co-administration phenoxodiol with doxorubicin synergistically inhibited the activity of SphK1 to suppress osteosarcoma cell growth both *in vivo* and *in vitro*.

Abbreviation: SphK1, sphingosine kinase-1; SKI-II, SphK1 inhibitor II; PARP, poly ADP ribose polymerase; OS, osteosarcoma; ASK1, apoptosis signal-regulating kinase 1; JNK, c-jun-NH2-kinase; PP1, protein phosphatase 1.

* *Corresponding author*. Tel./fax: +86 25 52238800 3377.
E-mail address: Zhangpinggu@gmail.com (Z. Gu).

1574-7891/$ – see front matter © 2012 Federation of European Biochemical Societies. Published by Elsevier B.V. All rights reserved.
doi:10.1016/j.molonc.2012.04.002

1. Introduction

For patients with osteosarcoma (OS), the use of chemotherapy has significantly improved survival from 11% with surgical resection alone in the 1960s, to 70% by the mid-1980s (Chou and Gorlick, 2006). Since then, despite significant advances in chemotherapies against OS in the past a few years, the survival of OS patients has not been much improved due to chemoresistance and other factors. As such, elucidation of the mechanisms of chemoresistance and implementation of strategies to overcome chemoresistance will be pivotal to improving survival for these patients.

The principal plant hormones flavonoids are known to possess diverse functional roles and to regulate plant cell apoptosis and cell cycle (Kandaswami et al., 2005). Many plant flavonoids show similar functional effects in animal and human cells, and are shown to be effective in inducing mitotic arrest and cell apoptosis in a number of cancer cells. Genistein, among all the flavonoids, has been proved to exert many anti-tumor effects (Kamsteeg et al., 2003; Lamartiniere et al., 1998), arguing that this molecule may offer novel approaches to cancer therapy (Banerjee et al., 2008; Sarkar and Li, 2003). Genistein is well tolerated in human, however, the clinical development of this agent has been compromised by the fact of its inability to achieve adequate plasma concentrations (Miltyk et al., 2003; Takimoto et al., 2003). As such, synthetic analogs of genistein are being developed for better anti-tumor efficacy. Of these genistein analogs, phenoxodiol is being assessed in several clinical studies against a range of cancer types and was shown to have a much better anticancer potency and efficacy in preclinical models and is less susceptible to metabolism compared with Genistein (Mor et al., 2006; Silasi et al., 2009).

The lipid kinase sphingosine kinase 1 (SphK1) catalyzes the phosphorylation of sphingosine to sphingosine-1-phosphate (S1P) (Shida et al., 2008; Vadas et al., 2008). *In vivo* and *in vitro* studies have proven that SphK1 is associated with cancer cell survival, proliferation, transformation, and prevention of apoptosis, the chemoresistance and angiogenesis (Shida et al., 2008; Vadas et al., 2008). Evidence from clinical samples demonstrates that SphK1 is over-expressed in many tumor types and that inhibitors of SphK1 may sensitize tumors to chemotherapeutic agents (Shida et al., 2008; Vadas et al., 2008). However, at least to our knowledge, the potential role of SphK1 in OS is largely missing. Though phenoxodiol is generally not known as a SphK1 specific inhibitor, phenoxodiol's major action, however, is believed to be blocking the activation of SphK1 (Gamble et al., 2006) (also see discussion in Shida et al., 2008). Our study here suggests that SphK1 might be a critical oncogene of OS and co-administration phenoxodiol with doxorubicin synergistically inhibited the activity of SphK1 to suppress osteosarcoma cell growth.

2. Materials and methods

2.1. Reagents

Phenoxodiol, doxorubicin, fumonisin B1, N-dimethylsphingosine, SKI-II and SP 600125 were obtained from Sigma (Sigma, St. Louis, MO); Anti-SphK1 (M-209, sc-48825), AKT1, tubulin, rabbit IgG-HRP and mouse IgG-HRP antibody were obtained from Santa Cruz Biotechnology (Santa Cruz, CA). p-SphK1 (Ser 225) antibody was obtained from Antibodies Online (ABIN265165, Shanghai, China). All other antibodies used in this study were purchased from Cell Signaling Technology (Beverly, MA).

2.2. Cell culture

Human osteosarcoma cell lines U2OS, MG-63, and SaOs-2 cells were cultured in Dulbecco's modified Eagle's medium (DMEM, Sigma, St. Louis, MO) containing 10% fetal calf serum (Sigma, St. Louis, MO), 2 mmol/L L-glutamine, and 100 mg/mL penicillin/streptomycin (Sigma, St. Louis, MO).

2.3. Live cell counting by trypan blue staining

Live OS cells after indicated treatment/s were determined by trypan blue staining assay and the % of live cell was calculated by the number of the trypan blue stained cells of treatment group divided by that of untreated control group.

2.4. Cell viability assay (MTT assay)

Cell viability was measured by the 3-[4,5-dimethylthylthiazol-2-yl]-2,5 diphenyltetrazolium bromide (MTT) method. Briefly, cells were collected and seeded in 96-well plates at a density of 4×10^5 cells/ml. 20 μl of MTT tetrazolium salt (Sigma, St. Louis, MO) dissolved in PBS at a concentration of 5 mg/ml was added to each well with indicated treatment and incubated in CO_2 incubator for 3 h at 37 °C. 150 μl of DMSO (Sigma, St. Louis, MO) was added to dissolve formazan crystals and the absorbance of each well was observed by a plate reader at a test wavelength of 490 nm.

2.5. Clonogenicity assay

U2OS cells (5×10^4) were suspended in 1 ml of DMEM containing 1% agar (Sigma, St. Louis, MO), 10% FBS and with indicated treatment/s or vehicle controls. The cell suspension was then added on top of a presolidified 1% agar in a 100 mm culture dish. The medium was replaced every 2 days. After 8 days of incubation, colonies were photographed at 4×. Colonies larger than 50 μm in diameter were quantified for number using Image J Software.

2.6. Western blotting

Cells were washed with ice-cold PBS, scraped into PBS, and collected by centrifugation. Pellets were re-suspended in a lysis buffer containing 50 mmol/L HEPES, 150 mmol/L NaCl, 1 mmol/L EDTA, 1 mmol/L EGTA, 10% glycerol, 0.5% NP-40, 0.5% Tween 20, 1 mmol/L dithiothreitol, and protease inhibitor cocktail (Roche Diagnostics, Indianapolis, IN) and vortexed for 20 min at 4 °C; insoluble material was removed by centrifugation. Proteins (30 μg) were resolved by SDS-PAGE and transferred to nitrocellulose membranes. Membranes were incubated sequentially in TBS containing 0.05% Tween-20

and 5% nonfat dry milk as follows: no addition, 1 h at room temperature (blocking); primary antibody, overnight at 4 °C; and secondary antibody (Amersham) diluted 1/4,000, 2 h at room temperature. Bound secondary antibody was detected by West Pico and West Femto chemiluminescent substrates (Pierce, Rockford, IL). Western blot results were quantified by Image J software from NIH website.

2.7. Immunoprecipitation (IP)

U2OS with indicated treatments were lysed with lysis buffer, 150 mM NaCl (pH 7.4), 1% Triton X-100, 10% glycerol, 0.3 mM EDTA, 0.2 mM Na3VO4, and protease inhibitor cocktails (Roche Diagnostics, Indianapolis, IN). Precleared samples (800 μg of protein each) were incubated with primary antibodies in lysis buffer overnight at 4 °C. To this was added 35 μl of protein A/G beads and the samples were incubated for 2 h at 4 °C. The beads were washed five times with phosphate-buffered saline (PBS) and twice with lysis buffer, boiled, followed by Western blots analysis.

2.8. Quantification of apoptosis by ELISA

The Cell Apoptosis ELISA Detection Kit (Roche, Palo Alto, CA) was used to quantify U2OS cell apoptosis according to manufacturer's protocol.

2.9. Caspase-3 activity assay

After indicated treatments, cytosolic proteins from approximately $2-3 \times 10^6$ U2OS cells were extracted in hypotonic cell lysis buffer (25 mm HEPES, pH 7.5, 5 mm $MgCl_2$, 5 mm EDTA, 5 mm dithiothreitol, 0.05% phenylmethylsulfonyl fluoride) by three cycles of freezing and thawing. The protein concentration of samples was determined by using a Bio-Rad Bradford protein assay kit (Bio-Rad, Shanghai, China). Ten micrograms of cytosolic extracts were added to caspase assay buffer (312.5 mm HEPES, pH 7.5, 31.25% sucrose, 0.3125% CHAPS) with benzyloxycarbonyl-DEVD-7-amido-4-(trifluoromethyl)coumarin as substrates (Calbiochem, Darmstadt, Germany). Release of 7-amido-4-(trifluoromethyl)coumarin (AFC) was quantified, after 2 h of incubation at 37 °C, using a Fluoroskan system (Thermo-Labsystems, Helsinki, Finland) set to an excitation value of 355 nm and emission value of 525 nm.

2.10. OS immunohistochemistry

The expression of SphK1 protein was performed on paraffin-embedded tumor sections (5 μm) mounted onto ChemMate Capillary Gap Microscope slides (Dako Cytomation, Milan, Italy), dried in a 45 °C oven for 12 h, deparaffinized in xylene, and rehydrated in graded alcohols and distilled water. Sections were heated in 10 mM citrate buffer pH 6.0 in a water bath at 96 °C for 45 min, cooled, and stored in PBS at pH 7.6. Endogenous peroxidase activity was blocked with 0.3% hydrogen peroxide for 10 min, followed by treatment with 10% BSA for 30 min. Sections were incubated overnight in a moist chamber at 4 °C with the primary antibodies anti-SphK1 (Cell Signaling). After washing in PBST, sections were incubated with secondary antibody and horseradish peroxidase conjugated with polymer for 30 min. Staining was visualized using 3-3′diaminobenzidine (Envision + Dual Link System-HRP, Dako Carpinteria, CA, USA) for 5 min, counterstained with Mayer's hematoxylin (Sigma Chemicals, St. Louis, MO, USA) for 1 min, dehydrated in a series of graded ethanol, cleared in xylene and mounted.

2.11. Sphingosine kinase activity assay

U2OS cells were collected and lysed by same lysis buffer for Western blots. After centrifuging at 13,000 × g for 60 min, proteins (100 μg) in supernatant were then incubated with 25 μM D-erythrosphingosine dissolved in 0.1% Triton X-100, 2 mM ATP, and [γ-32P] ATP (3.7×10^5 Bq dissolved in 20 mM $MgCl_2$) for 30 min at 37 °C in a final volume of 200 μl. The reaction was stopped by adding 20 μl of HCl (1 N), followed by 800 μl of chloroform/methanol/HCl (100:200:1, v/v). After vigorous vortexing, 250 μl of chloroform and 250 μl of KCl (2 M) were added, and phases were separated by centrifugation. The organic layer was dried and resuspended in chloroform/methanol/HCl 37% (100:100:0.2, v/v). Lipids were resolved on silica TLC plates in 1-butanol/acetic acid/water (3:1:1, v/v). Labeled S1P spots were visualized by autoradiography and quantified by scraping and counting in a scintillation counter. Sphingosine Kinase activity was valued as pmol/h/g protein is expressed as percentage of the untreated control. Each measurement was done in triplicate.

2.12. Enzymatic measurement of ceramide levels

Aliquots of the chloroform phases from cellular lipid extracts mentioned above were resuspended in 7.5% (w/v) octyl-β-D-glucopyranoside/5 mM cardiolipin in 1 mM DETPAC/10 mM imidazole (pH 6.6). The enzymatic reaction was started by the addition of 20 mM DTT, 0.88 U/ml *Escherichia coli* DAG kinase, 5 μCi/10 mM [γ-^{32}P]-ATP and the reaction buffer (100 mM imidazole (pH 6.6), 100 mM NaCl, 25 mM $MgCl_2$, and 2 mM EGTA). After incubation for 1 h at room temperature, lipids were extracted with chloroform/methanol/HCl (100:100:1, v/v) and 1 M KCl. [γ-^{32}P]-ceramide phosphate was resolved by TLC with chloroform/acetone/methanol/acetic acid/water (10:4:3:2:1, v/v) and quantified with a phosphorimager (Storm, Amersham). Known amounts of bovine ceramide standards were included in each assay. Ceramide levels are valued as fmol by nmol of phospholipid (PL) levels and are expressed as percentage of the untreated control. Each measurement was done in triplicate.

2.13. Generation of stable SphK1 knockdown U2OS cells by lentiviral transfection

U2OS cells were seeded in a 6-well plate 1 day prior to transfection and cultured to 50% of confluence the following day in 10% FBS medium with anti-biotic and polybrene. 10 μl/ml of lentiviral particles containing SphK1 shRNA (sc-44114-V, Santa Cruz Biotech, Santa Cruz, CA) were added to the cells for 48 h, cell culture medium then is replaced by fresh medium and cells were cultured for another 24 h, stable clones expressing SphK1 shRNA were selected by puromycin (1 μg/ml). Cell culture medium was replaced with fresh

puromycin-containing medium every 3 days, until resistant colonies can be identified. The expression level of SphK1 was detected by Western blots in the resistant colonies.

2.14. Generation of a stable SphK1 over-expression U2OS cell line by lentiviral transfection

A stable SphK1 over-expression U2OS cell line was generated by "Shanghai Genomics" (Shanghai, China) according to the protocols, briefly, WT SphK1 cDNA was introduced to pLKO.1 vector system, the vector was then transfected to U2OS cells with lentivirus and stable colons were again selected by puromycin. Expression level of SphK1 vs. their vector control clones was verified by Western blots.

2.15. Generation of a stable CA-Akt U2OS cells and ASK1/SphK1 RNAi transfection

U2OS were seeded in a 6-well plate 1 day prior to transfection and cultured to 60% of confluence the following day in 1% FBS medium. 2 μg of CA-Akt1 plasmids (constitutively active AKT1, addgene, Cambridge, MA) or vector control was diluted in 90 μl of DMEM at room temperature. Then, 4.0 μl of Lipofectamine2000 (Invitrogen, Carlsbad, CA) was then added, after 30 min, the complex was added to the well containing 1 ml of medium. Stable clones were selected by puromycin. ASK1 (obtained from Santa Cruz antibodies, SC, CA) or SphK1 siRNA (GGGCAAGGCCUUGCAGCUCdTT and GAGCUGCAAGGCCUUGCCCdTT, obtained from Qiagen, Shanghai, China) and scramble controls were transfected using same methods.

2.16. Mice OS xenograft models

CB.17 severe combined immuno-deficient (SCID) male mice (4–6 weeks old) were maintained at the animal facilities of Nanjing Medical University and handled according to institutional regulations, under sterile conditions in cage micro isolators. Mice was injected subcutaneously (s.c.) into the right flank with 1.5×10^6 U2OS cells in 0.1 ml DMEM. When the right flank xenografts were established at about 500 mm^3, the animals (5 mice per group) were treated daily with doxorubicin (1 mg/kg, i.p.), phenoxodiol (10 mg/kg, p.o.) or both for 16 days before sacrifice. Xenograft diameters were measured every 4 days using calipers. Tumor volumes (V) were calculated using the following formula: $V = A \times B^2/2$ (A = largest diameter; B = smallest diameter).

2.17. Statistical analysis

Individual experiment was analyzed separately (no pooling of samples was used). In each experiment, a minimum of three wells/dishes of each treatment was used. Each experiment was repeated a minimum of three times. In each experiment, the mean value of the repetitions was calculated and this value was used in the statistical analysis. All data were normalized to control values of each assay and are presented as mean ± standard deviation (SD). Data were analyzed by one-way ANOVA followed by a Scheffe's f-test by using SPSS software. $p < 0.05$ is considered statistically significant.

3. Results

3.1. Induction of apoptosis and inhibition of human osteosarcoma (OS) cell growth by phenoxodiol

In order to determine whether phenoxodiol conveys anti-proliferative effects on OS cells, we tested this isoflavone analog in three different OS cells (U2OS, MG-63 and SaOs-2 cells). Exponentially growing cells were exposed to increasing concentrations of phenoxodiol for 48 h, thereafter cell growth was measured by cell viability (MTT dye) assay. As shown in Figure 1A, in all three cell lines tested, phenoxodiol inhibited cancer cell growth at dose range from 1 to 20 μg/ml. 0.1 μg/ml of phenoxodiol failed to inhibit OS cell growth (Figure 1A). Phenoxodiol also dose-dependently induced U2OS cell death as evidenced by decreased number of live cells and surviving colonies after treatment (Figure 1B). Caspase-3 activity and Histone-DNA ELISA OD were also increased by phenoxodiol, indicating cell apoptosis (Figure 1C). These data suggest that phenoxodiol by itself was able to induce cell apoptosis and inhibit cell growth in human OS cells. However, the effect of phenoxodiol was generally moderate. 5 μg/ml of phenoxodiol only reduced U2OS cell viability ~20% (Figure 1A), led to around ~20% cell death (Figure 1B) and increased caspase-3 activity to 2.20 fold (Figure 1C). We decided to choose this concentration of phenoxodiol to sensitize doxorubicin.

3.2. Phenoxodiol and doxorubicin synergistically inhibit OS cell growth and induce apoptosis

The main goal of this study is to test the chemo-sensitization effect of phenoxodiol on doxorubicin in OS cells. To test this hypothesis, we used cell viability MTT OD to reflect OS cell growth; we also used Histone DNA ELISA and caspase-3 assay to test cell apoptosis. Results in Figure 2 show that treatment OS cells with either phenoxodiol (5 μg/ml) or doxorubicin (0.25 μM) alone produced a relative moderate effect on cell growth inhibition (Figure 2A) and apoptosis (Figure 2B). Only the group that received both phenoxodiol and doxorubicin treatments showed significant reduced cancer cell growth and enhanced apoptosis (Figure 2A,B). The U2OS cell viability reduced to 18% after phenoxodiol and doxorubicin co-administration after four days, compared to 79% after phenoxodiol only treatment and 67% after doxorubicin only treatment (Figure 2A). These results suggest that phenoxodiol and doxorubicin synergistically inhibit OS cell growth and induce apoptosis.

3.3. Phenoxodiol facilitates doxorubicin induced mitochondrial apoptosis pathway to inhibit U2OS cell growth

Activation of mitochondrial apoptosis pathway is critical for doxorubicin induced OS cell growth inhibition and cell death (Park et al., 2011; Zhu et al., 2011). Facilitating the induction of this pathway has been proven to be effective to sensitize doxorubicin (Park et al., 2011; Zhu et al., 2011). As expected, here we found that doxorubicin treatment increased

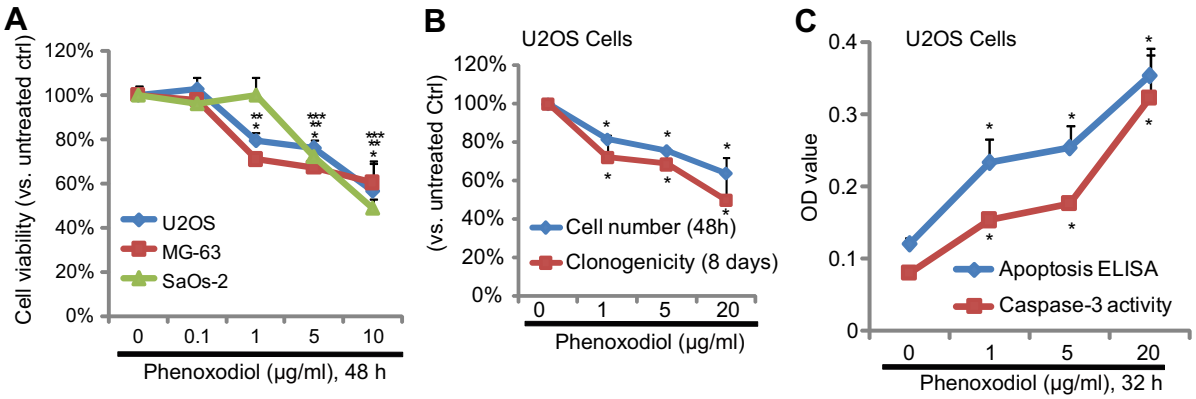

Figure 1 – Induction of apoptosis and inhibition of human osteosarcoma (OS) cell growth by phenoxodiol. (A) U2OS, MG-63 and SaOs-2 cells were either left untreated or exposed to indicated concentration of phenoxodiol for 48 h; cell viability was analyzed by MTT dye assay and was normalized to the OD value of untreated control. (B) Live U2OS cells and colonies after indicated phenoxodiol treatment were calculated using methods as described in the Materials and methods. Results were normalized to untreated control group. (C) Histone DNA ELISA and caspase-3 activity were utilized to analyze U2OS cell apoptosis after 32 h of indicated phenoxodiol treatments. The data in this figure were representatives of more than 3 different experiments. The values in the figures are expressed as the means ± standard deviation (SD). *$p < 0.05$ vs. untreated control group for U2OS cells (A–C). **$p < 0.05$ vs. untreated control (MG-63 cells). ***$p < 0.05$ vs. untreated control (SaOs-2 cells).

caspase-3 and poly ADP ribose polymerase (PARP) cleavage (Figure 3A) as well as cytosol cytochrome C release (Figure 3B), phenoxodiol significantly promoted these processes (Figure 3A,B). The general caspase inhibitor Z-VAD-FMK significantly diminished growth inhibition by phenoxodiol and doxorubicin co-administration (Figure 3C), suggesting that phenoxodiol facilitates doxorubicin-induced mitochondrial apoptosis pathway to inhibit U2OS cell growth.

3.4. *Inhibition of SphK1 sensitizes doxorubicin induced U2OS cell growth suppression*

As we discussed early, SphK1 activation promotes cancer cell growth and protects of cells from apoptosis (Maceyka et al., 2002). Studies have reported that phenoxodiol induce cell cycle arrest and growth inhibition mainly through suppression of SphK1 activity (Gamble et al., 2006; Sabbadini, 2006; Vadas et al., 2008), SphK1 activity was tested in OS cells after phenoxodiol and doxorubicin treatments. Results in Figure 4A showed that both phenoxodiol and doxorubicin treatment inhibited SphK1 activity, combination of the two further reduced the activity of SphK1 (Figure 4A, upper panel). Western-blots results in Figure 4A (lower panel) further demonstrated that phenoxodiol and doxorubicin synergistically reduced the phosphorylation of SphK1 (Ser 225), an indicator of SphK1 activation (Hait et al., 2005; Okada et al., 2009; Paugh et al., 2008), note that total SphK1 level was not changed (Figure 4A, lower panel). To test whether inhibition of SphK1 could sensitize doxorubicin in U2OS cells, we created a stable U2OS cell line expressing SphK1 shRNA by lentiviral transfection (See Materials and methods), Western-blots results in Figure 4B confirmed knocking down of SphK1 in the stable cell lines (16% of control cell level). To further confirm the specificity of the SphK1 antibody used in this study, we obtained siRNAs for human SphK1 (GGGCAAGGCCUUGCAGCUCdTT and GAGCUGCAAGGCCUUGCCCdTT). U2OS Cells

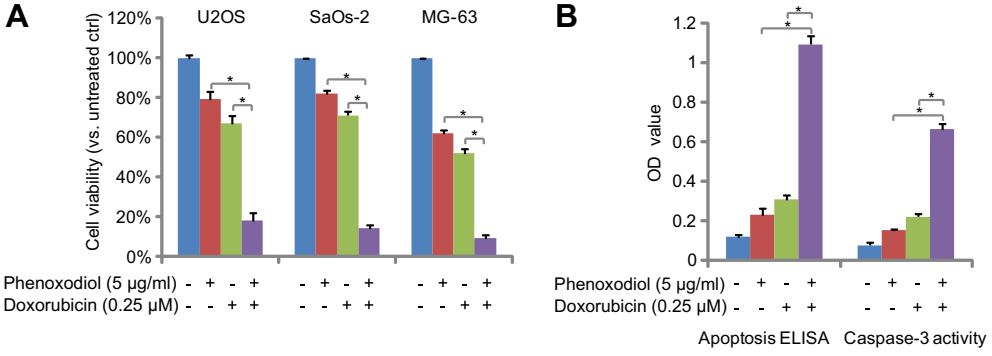

Figure 2 – Phenoxodiol and doxorubicin synergistically inhibit OS cell growth and induce apoptosis. (A) U2OS, MG-63 and SaOs-2 cells were either left untreated or exposed to indicated dose of phenoxodiol, doxorubicin or both for 48 h; cell viability was analyzed by MTT dye assay and normalized to untreated control group. (B) The apoptosis of U2OS cells after 32 h of phenoxodiol, doxorubicin or combination treatment/s was reflected by Histone-DNA ELISA (apoptosis ELISA) and caspase-3 activity. The data in this figure were representatives of more than 3 different experiments. The values in the figures are expressed as the means ± standard deviation (SD). *$p < 0.05$.

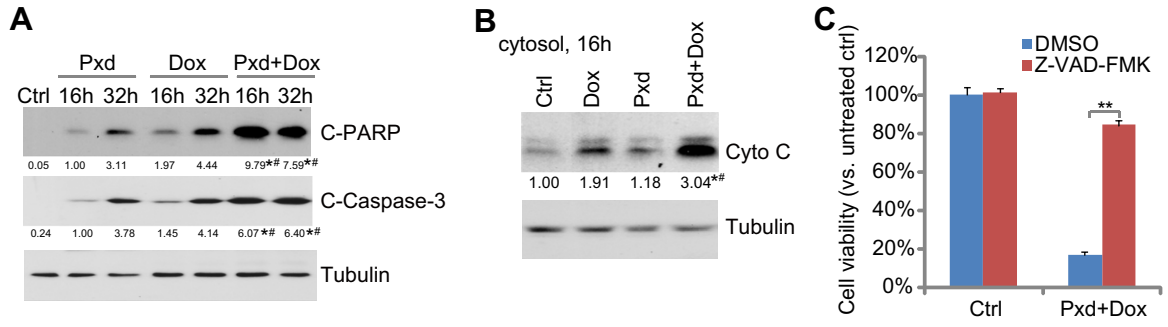

Figure 3 – Phenoxodiol facilitates doxorubicin induced mitochondrial apoptosis pathway to inhibit U2OS cell growth. U2OS cells were either left untreated (Ctrl) or exposed to phenoxodiol (Pxd, 5 μg/ml), doxorubicin (Dox, 0.25 μM) or both (Pxd + Dox) for indicated hours, followed by Western blots detecting cleaved-Caspase-3 (C-caspase-3), cleaved-PARP (C-PARP), cytosol-Cytochrome C (A–B). MTT dye assay was utilized to analyze cell viability of phenoxodiol plus doxorubicin (Pxd, 5 μg/ml + Dox, 0.25 μM, 48 h) treated U2OS cells with or without Z-VAD-FMK (50 μM). Western blots results were quantified by Image J software after normalized to tubulin and were expressed as fold change vs. the lane marked as "1.00". The data in this figure were representatives of 3 different experiments. The values in the figures are expressed as the means or with standard deviation (SD). *$p < 0.05$ vs. phenoxodiol treatment group. #$p < 0.05$ vs. doxorubicin treatment group. **$p < 0.05$.

were transfected SphK1 siRNA with Lipofectamine2000. Results in Figure 4B (lower panel) showed that SphK1 siRNA dose-dependently reduced the level of SphK1. Doxorubicin induced cell viability loss was significantly diminished in the SphK1 knockdown stable cells (Figure 4C). Further, two SphK1 inhibitors N-dimethylsphingosine (DMS) and SphK1 inhibitor II (SKI-II) significantly enhanced doxorubicin-induced U2OS cell viability loss (Figure 4D), suggesting that SphK1 suppression sensitizes doxorubicin-induced U2OS cell growth inhibition.

3.5. *Identification SphK1 as a potential oncogene in OS*

As we discussed early, over-expression of SphK1 is commonly seen in a number of cancers, and is associated with cancer progression. SphK1 also helps cancer cell transformation and tumor angiogenesis (Sabbadini, 2006; Vadas et al., 2008). Functionally, SphK1 produces sphingosine-1-phosphate (S1P) that functions as an extracellular ligand for the receptor S1P Receptor (S1PR), or intracellular second message, leading to the activation of various signaling cascades and multiple key processes that are involved in cancer development and progression (Sabbadini, 2006; Vadas et al., 2008). However, the expression level of SphK1 and its potential role in OS are largely unknown. Here, our Western blots and immunohistochemistry results demonstrated that SphK1 is also over-expressed in multiple clinical OS tissues (Figure 5A,B). To further investigate the role of SphK1 in OS cell progression, we were able to generate a stable U2OS cell line over-expressing SphK1 (see Materials and methods) (Figure 5C). We found that these stable cells with over-expressed SphK1 grew faster than vector-transfected control U2OS cells (Figure 5D). SphK1 over-expression also protected U2OS cells from cell viability loss and cell death induced either by doxorubicin or with phenoxodiol (Figure 5E and F). These data suggest that, just like many other cancers, over-expression of SphK1 in OS might contribute to tumor cell growth and apoptosis escape, and SphK1 might be a critical oncogene in OS.

3.6. *Phenoxodiol and doxorubicin synergistically increase intracellular level of ceramide*

It has been known that inhibition of SphK1, either by pharmacological inhibitors or by downregulation manipulation, enhances intracellular ceramide production and promotes cell apoptosis (Alemany et al., 2007; Maceyka et al., 2002). On the other hand, over-expression of SphK1 reduced the level of sphingosine, ceramide and apoptosis (Shida et al., 2008). Further, cytosolic S1P formed by SphK1 inhibits ceramide biosynthesis to further reduce ceramide level and apoptosis (Maceyka et al., 2002). Since we have shown that phenoxodiol and doxorubicin synergistically inhibited SphK1 activity (Figure 5), we then tested intracellular level of ceramide in U2OS cells after treatment with doxorubicin, phenoxodiol or both. Results in Figure 6A demonstrated that phenoxodiol and doxorubicin synergistically increased intracellular level of ceramide in U2OS cells. Fumonisin B1, a ceramide synthase inhibitor (Merrill et al., 1993), largely inhibited ceramide accumulation. The fact that over-expression of SphK1 reversed ceramide increase by the co-administration suggesting that SphK1 inhibition is the main cause of ceramide increase by phenoxodiol and doxorubicin co-administration (Figure 6B). (Also see signaling pathway Figure 10).

3.7. *Increased intracellular ceramide level by phenoxodiol and doxorubicin deactivates Akt*

Studies have confirmed that increased intracellular level of ceramide can activate serine/threonine phosphatase 1 (PP1) to de-phosphorylate AKT, contributing to cell growth inhibition and apoptosis (Dobrowsky et al., 1993; Law and Rossie, 1995; Wolff et al., 1994; Zhu et al., 2011). We then studied phenoxodiol and doxorubicin co-administration on Akt activation in U2OS cells. Treatment either with phenoxodiol or doxorubicin had minor effects on Akt and downstream GSK3 phosphorylation, while a combination of these two resulted in a significant decrease of Akt/GSK3 phosphorylation

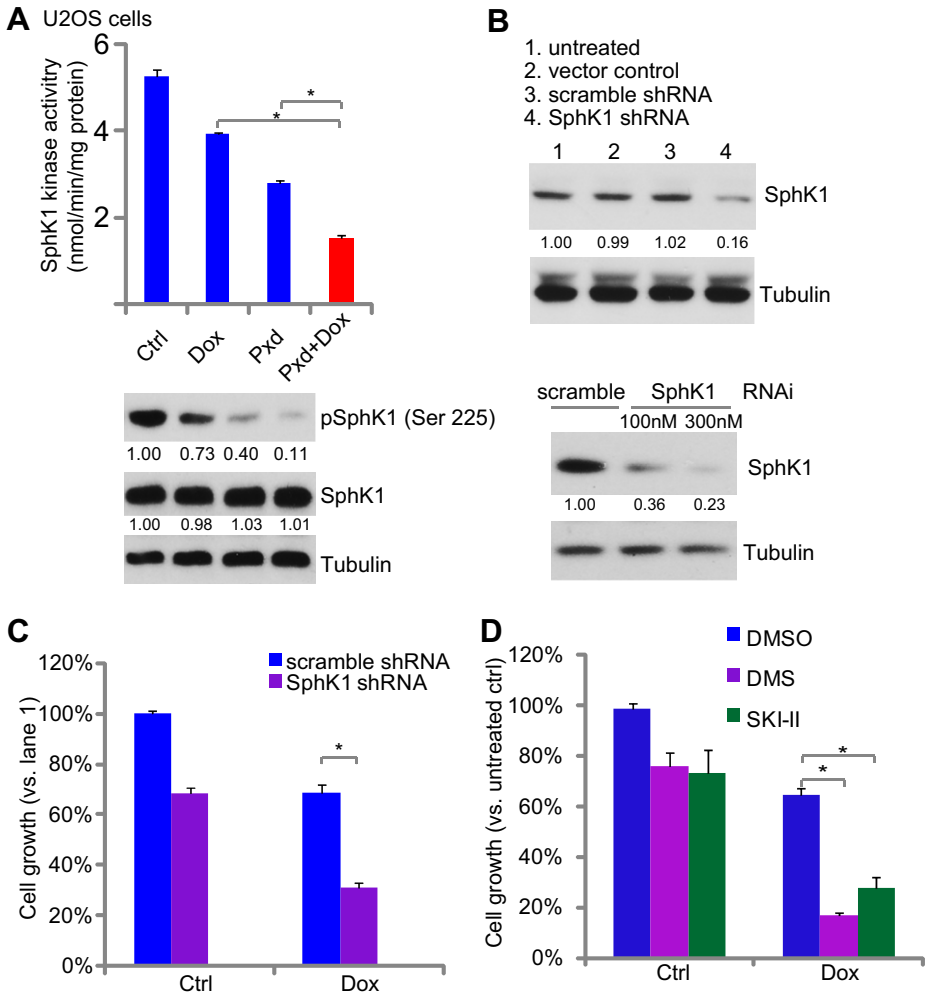

Figure 4 – Inhibition of SphK1 sensitizes doxorubicin induced U2OS cell growth suppression. U2OS cells were either left untreated (Ctrl) or exposed to phenoxodiol (Pxd, 5 μg/ml), doxorubicin (Dox, 0.25 μM) or both (Pxd + Dox) for 24 h, SphK1 kinase activity was analyzed as described (A, upper panel), phosphorylation and total level of SphK1 were also tested by Western blots (A, lower panel). Lentiviral particles containing SphK1 shRNA or scramble shRNA control were introduced to U2OS cells as described, stable cell lines were selected by puromycin, expression level of SphK1 and tubulin was measured by Western blots (B, upper panel). U2OS cells were transfected with scramble siRNA (300 nM) or indicated concentration of SphK1 siRNA by Lipofectamine2000 for 48 h, followed by Western-blots detecting expression level of SphK1 (B, lower panel). Same number of stable SphK1 shRNA transfected U2OS cells and the scramble shRNA transfected control cells were exposed to doxorubicin (Dox, 0.25 μM) for 48 h, cell viability was analyzed by MTT assay (C). Effect of N-dimethylsphingosine (DMS, 10 μM) or SphK1 inhibitor II (SKI-II, 20 μM) on doxorubicin (Dox, 0.25 μM)-induced U2OS cell viability (48 h) was shown in (D). The data in this figure were representatives of more than 3 different experiments, similar results were obtained. The values in the figures are expressed as the means ± standard deviation (SD) except for A. *$p < 0.05$ vs. scramble shRNA transfected cells.

(Figure 7A). Co-immunoprecipitation (Co-IP) experiments in Figure 7B demonstrated that phenoxodiol and doxorubicin synergistically enhanced PP1-Akt association. Ceramide synthase inhibitor fumonisin B1 diminished Akt inhibition by co-administration (Figure 7C), indicating that increased intracellular level of ceramide by phenoxodiol and doxorubicin co-administration promotes PP1/Akt association to dephosphorylate Akt. The fact that construction of a constitutively active Akt1 (CA-Akt) expressing stable U2OS cells (see Materials and methods) restored Akt activation and showed resistance of cell growth inhibition by the co-administration suggested that Akt inhibition is involved in cell growth inhibition by phenoxodiol and doxorubicin co-administration (Figure 7D–E).

3.8. *Phenoxodiol and doxorubicin synergistically promote JNK activation*

Another well-established downstream signal target of ceramide is JNK (Basu and Kolesnick, 1998; Verheij et al., 1996), ceramide-initiated JNK signaling is required for stress-induced apoptosis (Verheij et al., 1996). Meanwhile, activation of JNK is also important to mediate doxorubicin-induced apoptosis in a number of cancer cells (Panaretakis et al., 2005; Yu et al., 2008). We then tested JNK activation in U2OS cells with phenoxodiol and doxorubicin treatment/s. As shown in Figure 8A, either phenoxodiol or doxorubicin caused a moderate but obvious JNK phosphorylation in U2OS cells,

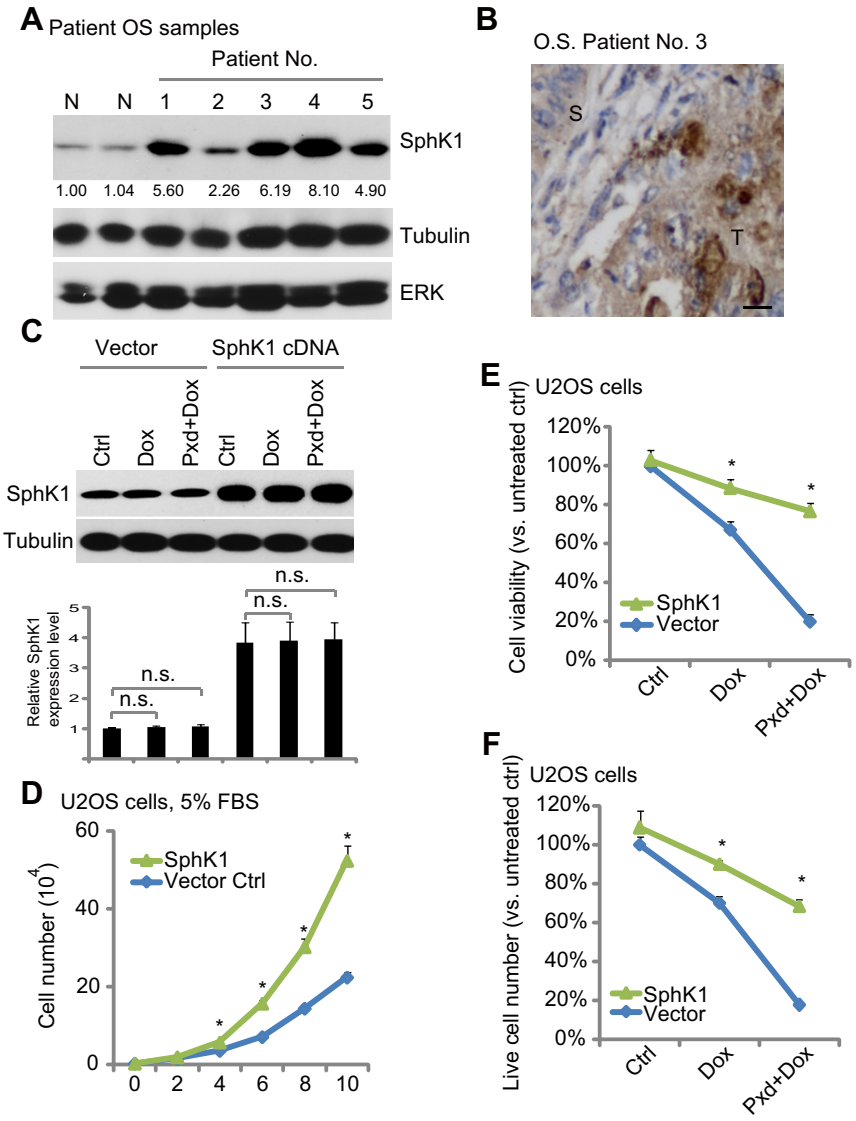

Figure 5 – Identification SphK1 as a potential oncogene in OS. Western blots results shows the expression level of SphK1 in fresh removed five clinical OS tissues from and 2 normal osteoblast tissues (N) (A). Immunohistochemistry results confirmed the up-regulation of SphK1 in OS patient (No. 3), T: Tumor tissue, S: surrounding normal tissue (B). The expression level of SphK1 after 24 h of doxorubicin (Dox, 0.25 μM) or plus phenoxodiol (Pxd, 5 μg/ml) (Pxd + Dox) treatment/s in SphK1 over-expression stable U2OS cells and their vector controls were examined by Western -blots, results were quantified by Image J software (C). 1 * 10^4 SphK1 over-expression stable U2OS cells and their vector controls were cultured in 15 cm culture dish with 5% FBS, total cell number in each dish was recorded every two days (D). Same number of SphK1 over-expression stable U2OS cells and their vector controls were also exposed to doxorubicin (Dox, 0.25 μM) or plus phenoxodiol (Pxd, 5 μg/ml) (Pxd + Dox) for 48 h, cell viability was analyzed by MTT dye assay (E) and live cell number was also recorded in (F). The data in this figure were representatives of more than 3 different experiments, similar results were obtained. The values in the figures are expressed as the means or with standard deviation (SD). *$p < 0.05$ vs. vector control cells. n.s.: no statistics difference.

combination of these two resulted in a significantly enhanced JNK activation. Western-blots results in Figure 8B showed that JNK phosphorylation by doxorubicin was enhanced by exogenously adding cell-permeable short chain ceramide (C6), and was largely reduced by fumonisin B1, suggesting that ceramide is required for JNK activation by doxorubicin. Phenoxodiol increases ceramide production (Figure 6) which leads to further JNK activation and cell death, the latter was supported by the fact that JNK inhibitor reduced cell death by phenoxodiol and doxorubicin co-administration (Figure 8C). To indentify the intermediate player for JNK activation, we found that Apoptosis Signal-Regulating Kinase 1 (ASK1) might be the key player (see Discussion), since siRNA knockdown of ASK1 significantly reduced JNK activation in U2OS cells (Figure 8D).

3.9. *Synergistic anti-OS effect of phenoxodiol and doxorubicin in mice xenograft model*

Finally, by using a mice U2OS OS xenograft model, we verified the synergistic anti-OS effect of phenoxodiol and doxorubicin

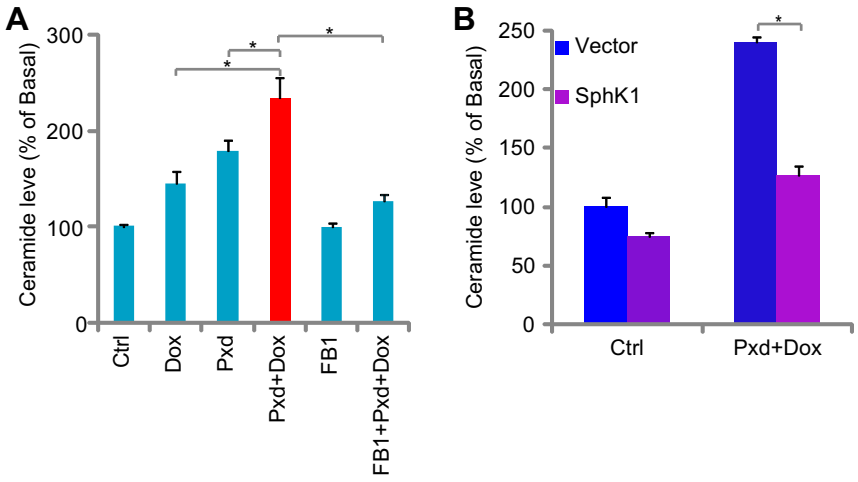

Figure 6 – Phenoxodiol and doxorubicin synergistically increase intracellular level of ceramide. Intracellular ceramide level of U2OS cells treated with 24 h of doxorubicin (Dox, 0.25 μM), phenoxodiol (Pxd, 5 μg/ml) or both (Pxd + Dox), with or without fumonisin B1 (10 μM) (FB1 + Pxd + Dox) were analyzed as described (A). SphK1 over-expression stable U2OS cells and their vector controls were exposed to doxorubicin (Dox, 0.25 μM) plus phenoxodiol (Pxd, 5 μg/ml) (Dox + Pxd) for 24 h, cellular ceramide level was analyzed in (B). The data in this figure were representatives of more than 3 different experiments, similar results were obtained. The values in the figures are expressed as the means ± standard deviation (SD). *$p < 0.05$.

in vivo. As shown in Figure 9A, only group that received both phenoxodiol and doxorubicin showed a significant reduced tumor growth. The group that received either single treatment showed slight anti-tumor growth effect as compared to vehicle controls (Figure 9A). Interestingly, stable SphK1 knockdown U2OS cells grew slowly compared to normal U2OS cells *in vivo*, while stable SphK1 over-expression U2OS cells grew faster to form bigger tumor mass (Figure 9B). These data provide *in vivo* evidence to support SphK1 as a potential oncogene of OS.

4. Discussion

In this current study, we argue that SphK1 might be a critical oncogene for OS; our argument is supported by the following evidences. First, SphK1 is over-expressed in multiple clinical OS tissues. Second, over-expression of SphK1 in OS cell line U2OS promoted its growth and conveyed the resistance against doxorubicin. Third, target shRNA knocking down of SphK1 suppressed OS cell growth and increased doxorubicin sensitivity. Fourth, inhibition of SphK1 by phenoxodiol suppressed OS cell growth and dramatically enhanced doxorubicin induced anti-OS effect. Finally, inhibition of SphK1 increased cellular level of ceramide to promote cancer cell apoptosis.

Many studies have demonstrated that ceramide plays key roles in the response of cancer cells to chemotherapeutic drugs (Ogretmen and Hannun, 2001; Reynolds et al., 2004). Ceramide has been shown to regulate anti-proliferative responses associated with cell apoptosis, growth arrest, differentiation and senescence in multiple human cancer cell lines (Ogretmen and Hannun, 2001; Reynolds et al., 2004). Many anti-cancer agents increase endogenous ceramide levels via the *de novo* pathway and/or the hydrolysis of sphingomyelin to promote apoptotic cancer cell death (Ogretmen and Hannun, 2001; Reynolds et al., 2004). At longer term, however, cancer cells are able to remove excess ceramide through diverse metabolic pathways (Babia et al., 1998; van Lummel et al., 2011). It has been suggested that agents that could increase intracellular ceramide accumulation would provide a pro-apoptosis outcomes (Ogretmen and Hannun, 2001; Reynolds et al., 2004).

Recent study by Ji et al. (2010) suggested exogenously adding cell permeable short-chain ceramide (C6) dramatically increased chemo-sensitivity of doxorubicin in multiple cancer cell lines *in vitro*, arguing that increasing cellular ceramide level would sensitized doxorubicin induced anti-tumor effect. The systematic use of short-chain ceramide is, however, limited due to its insolubility to water. As such, nanomaterials have been developed for better systematically deliver of short-chain ceramide (Liu et al., 2010; Tagaram et al., 2011; van Lummel et al., 2011), however, even with the help of nanomaterials, a relatively high concentration of ceramide (20–50 mg/kg) is often needed to achieve anti-cancer effect along with the possible side effects of nanomaterials (Liu et al., 2010; Tagaram et al., 2011; van Lummel et al., 2011). An alternative way to sensitize doxorubicin is to increase intracellular ceramide level endogenously. One of the key kinases that regulate the balance between ceramide and S1P is SphK1. Inhibitors against SphK1 suppress the phosphorylation of sphingosine to S1P to increase sphingosine and ceramide level (Reynolds et al., 2004; Shida et al., 2008; Vadas et al., 2008). In the current study, we found that phenoxodiol inhibited SphK1 activity to facilitate ceramide production and sensitized OS cells to doxorubicin. Co-administration of phenoxodiol and doxorubicin led a significant inhibition of OS cell growth both *in vitro* and in mice xenograft models.

Activation of PI3K/Akt signaling has been associated with OS progression. A recent study suggested inhibition of PI3K/Akt signaling pathway by Grifolin induces apoptosis in human

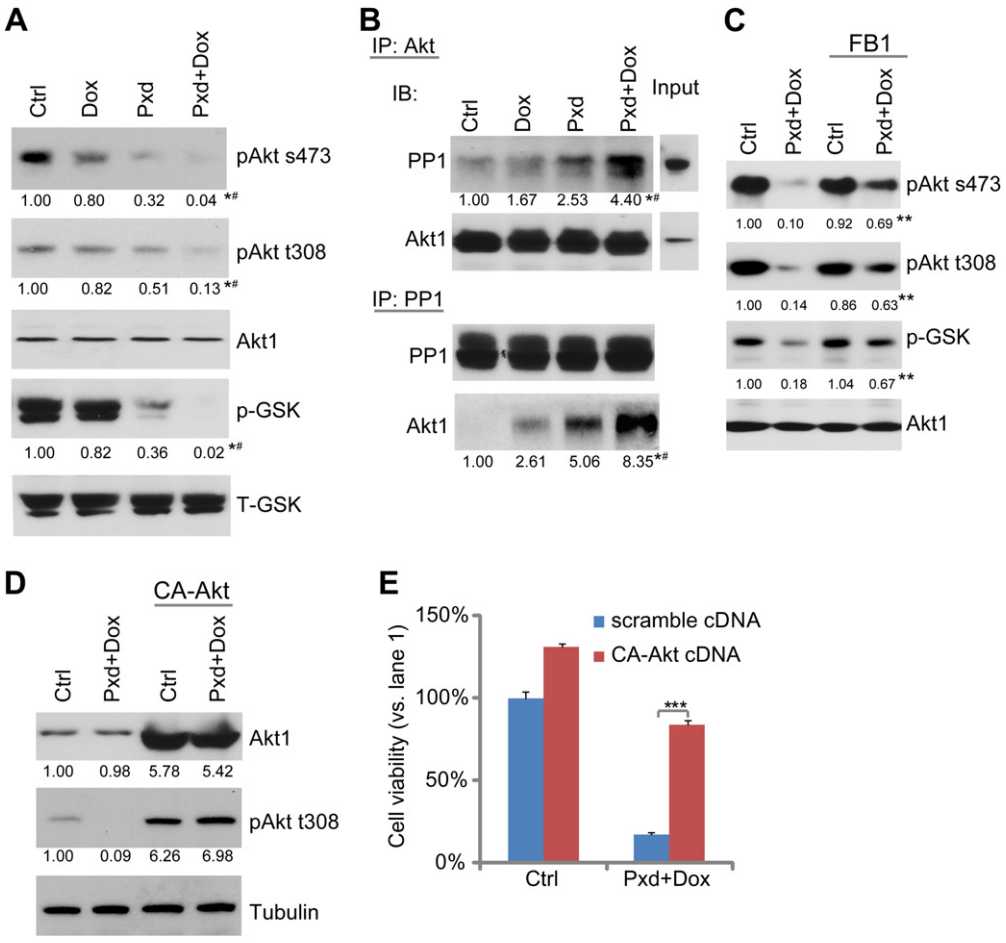

Figure 7 – Increased intracellular ceramide level by phenoxodiol and doxorubicin deactivates Akt. Phosphorylation of Akt (Thr 308 and ser 473) and GSK3 (α/β, S21/9) and corresponding loading controls in U2OS cells after 24 h exposure of doxorubicin (Dox, 0.25 μM), phenoxodiol (Pxd, 5 μg/ml) or both was detected by Western blots, Akt and GSK3 phosphorylation levels were normalized to untreated control (A). The association between PP1 and Akt was also examined using Co-IP experiments mentioned above (B). (C) Western blots detecting Akt and GSK3 phosphorylation in untreated U2OS cells or Dox + Pxd (24 h) treated cells in the presence or absence of fumonisin B1 (10 μM). CA-Akt cDNA or vector control was transfected into U2OS cells, Dox + Pxd (24 h)'s effect on Akt phosphorylation and cell viability were tested by Western blots (D) and MTT dye assay (E) separately. Notable blots were quantified by Image J software after normalized to tubulin and were expressed as fold change vs. the lane marked as "1.00". The data in this figure were representatives of more than 3 different experiments, similar results were obtained. *$p < 0.05$ vs. Dox only group. #$p < 0.05$ vs. Pxd only group. (A–C). **$p < 0.05$ vs. lane 2 (C). ***$p < 0.05$ (E).

osteosarcoma cells (Jin et al., 2007). Celecoxib, a cyclooxygenase-2 inhibitor, also induces apoptosis in human osteosarcoma cell via down-regulation of PI3K/Akt (Liu et al., 2008). Activation of this pathway has also been linked to chemoresistance, and inhibition of the Akt signaling sensitizes of multidrug resistant human ostesarcoma cells to Apo2 Ligand/TRAIL-induced apoptosis (Cenni et al., 2004). In the current study, we found that phenoxodiol and doxorubicin synergistically increased cellular level of ceramide, which promoted the association between Akt and phosphatase PP1 to dephosphorylate Akt. Introducing a constitutively active Akt (CA-Akt) restored Akt activation and diminished cell growth inhibition by co-administration, suggesting that to ceramide mediated Akt inactivation contributes to the anti-OS effect by phenoxodiol and doxorubicin.

Another well known downstream kinase of ceramide is JNK (Verheij et al., 1996). Since phenoxodiol and doxorubicin synergistically increased ceramide production, it was not surprised to see a significant JNK activation after co-administration. The fact that JNK inhibitor diminished growth inhibition by co-administration supports that JNK activation also contributes to the process. Among MAPKKKs, ASK1 is known to be activated in response to various cytotoxic and induce JNK activation and apoptosis (Tobiume et al., 2001). Previous studies have demonstrated that over-expression of wild-type or constitutively active ASK1 (CA-ASK1) induce apoptosis while kinase-inactive or dominant negative mutant of ASK1 inhibits apoptosis by various stresses (Tobiume et al., 2001). Interestingly, studies have suggested that ceramide can also cause ASK1 activation to activate JNK signaling cascade (Kolesnick and Kronke, 1998; Tobiume et al., 2001). To examine the possible role of ASK1 as an upstream MAP kinase in regulating JNK activation by phenoxodiol and doxorubicin, we used RNAi to knockdown ASK1, we found that phenoxodiol

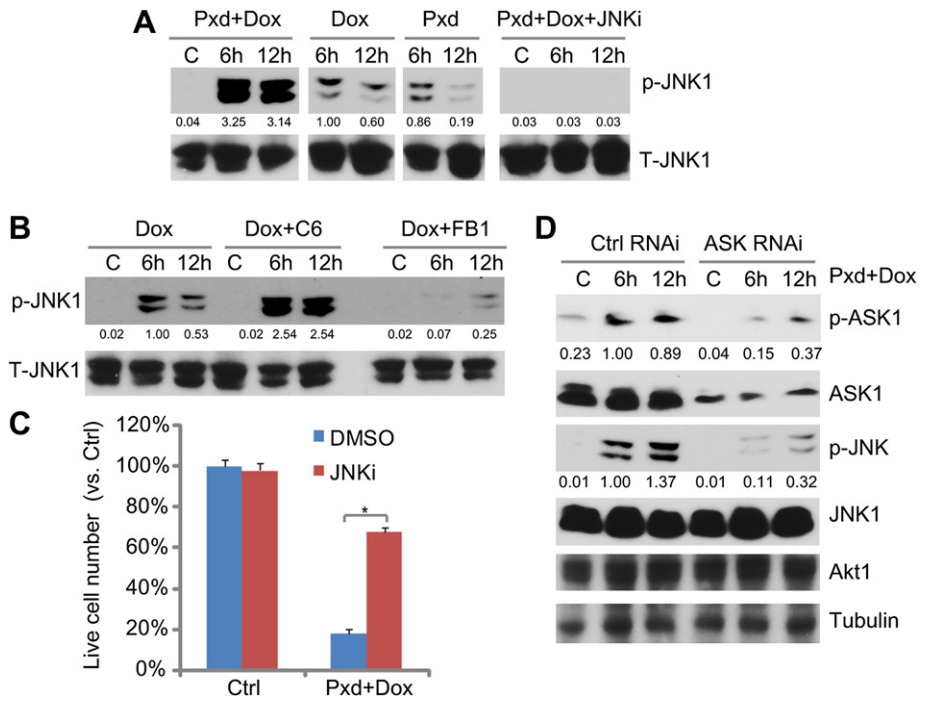

Figure 8 – Phenoxodiol and doxorubicin synergistically promote JNK activation. Phosphorylation and non-phosphorylation level of JNK in U2OS cells after indicated exposure of doxorubicin (Dox, 0.25 μM), phenoxodiol (Pxd, 5 μg/ml) or both were detected by Western blots, JNK activation was quantified and normalized to Dox only 6 h time point (JNKi: SP 600125, 2 μM, 1 h pretreatment) (A). U2OS cells were pretreated with C6 ceramide (C6, 10 μg/ml) or fumonisin B1 (FB1, 10 μM) for 2 h, followed by doxorubicin (Dox, 0.25 μM) exposure for indicated time, phosphorylation and non-phosphorylation expression levels of JNK were detected (B). Effects of JNK inhibitor SP 600125 (2 μM) on doxorubicin (Dox, 0.25 μM) and phenoxodiol (Pxd, 5 μg/ml) co-administration-induced U2OS cell death were reflected by reduced live cell number (C). ASK1 RNAi or scramble control RNAi (300 nM each) was transfected to U2OS cells (48 h transfection), successfully transfected cells were confirmed by Western blots and used to test activation of JNK after co-administration (D). JNK, ASK1 phosphorylation was quantified and normalized to Ctrl RNAi 6 h group (lane 2). The data in this figure were representatives of 3 different experiments, similar results were obtained. *$p < 0.05$.

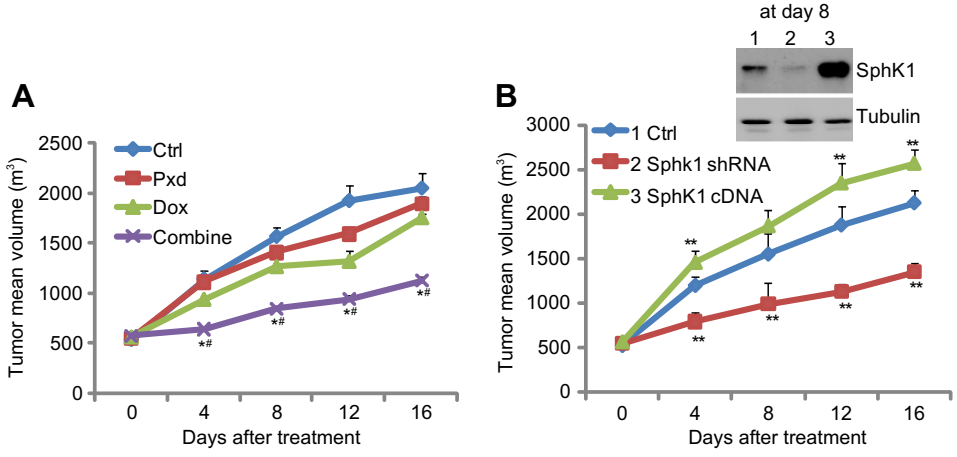

Figure 9 – Synergistic anti-OS effect of phenoxodiol and doxorubicin in mice xenograft model. The U2OS cell xenografted mice (5 mice per group) were either left untreated or treated with daily with either doxorubicin (1 mg/kg, i.p.), phenoxodiol (10 mg/kg, p.o.) or both for 16 days, tumor size was measured every 4 days (see Materials and methods for detail) (A) $1 * 10^6$ normal, SphK1 over-expression stable U2OS cells or SphK1 shRNA knocking-down stable U2OS cells were xenografted to SCID mice, tumor growth was monitored every 4 days for a total of 16 days, tumor size was monitored, tumors at day 8 were also surgically removed, and the expression level of SphK1 was tested by Western blots (B). The data in this figure were representatives of more than 2 different experiments, similar results were obtained. *$p < 0.05$ vs. doxorubicin only group (A), #$p < 0.05$ vs. phenoxodiol only group (A). **$p < 0.05$ vs. Ctrl cell group (B).

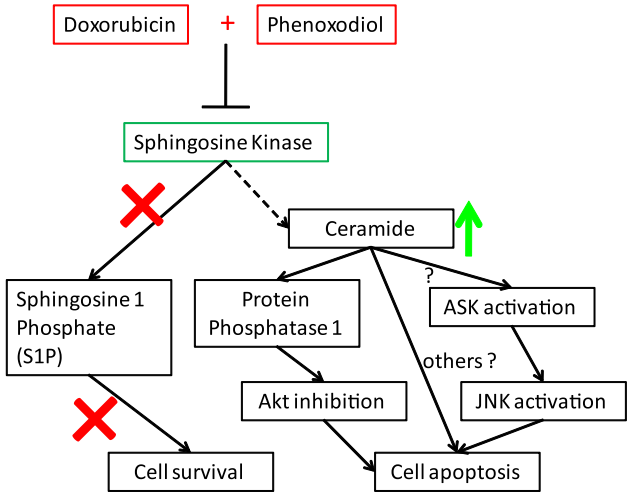

Figure 10 – Proposed signaling pathways involved in this study. SphK1 is a potential key oncogene for OS. Phenoxodiol and doxorubicin synergistically inhibited SphK1 activity to increase ceramide production. Increased ceramide then induces PP1/Akt association to deactivate Akt, ceramide also activates ASK1/JNK pathway, Akt inactivation, JNK and possible other uncharacterized mechanisms together mediate OS cell growth inhibition and apoptosis.

and doxorubicin co-administration induced a significant ASK phosphorylation (an indicator of its activation), RNAi-mediated ASK1 knockdown dramatically reduced JNK activation by the co-administration. These results suggest that phenoxodiol and doxorubicin co-administration activates ASK1/JNK signaling cascade to mediate cytotoxicity and apoptosis. However, how JNK activation is regulated by ASK1, and how the co-administration or ceramide activates ASK1 deserves further investigations.

5. Conclusion

Finally, we conclude that SphK1 might be a critical oncogene for OS. Co-administration phenoxodiol with doxorubicin synergistically inhibit the activity of SphK1 to suppress osteosarcoma cell growth both *in vivo* and *in vitro*. Ceramide accumulation, JNK activation and Akt inhibition might be involved in this process.

REFERENCES

Alemany, R., van Koppen, C.J., Danneberg, K., Ter Braak, M., Meyer Zu Heringdorf, D., 2007. Regulation and functional roles of sphingosine kinases. Naunyn. Schmiedebergs. Arch. Pharmacol. 374, 413–428.

Babia, T., Veldman, R.J., Hoekstra, D., Kok, J.W., 1998. Modulation of carcinoembryonic antigen release by glucosylceramide – implications for HT29 cell differentiation. Eur. J. Biochem. 258, 233–242.

Banerjee, S., Li, Y., Wang, Z., Sarkar, F.H., 2008. Multi-targeted therapy of cancer by genistein. Cancer Lett. 269, 226–242.

Basu, S., Kolesnick, R., 1998. Stress signals for apoptosis: ceramide and c-Jun kinase. Oncogene 17, 3277–3285.

Cenni, V., Maraldi, N.M., Ruggeri, A., Secchiero, P., Del Coco, R., De Pol, A., Cocco, L., Marmiroli, S., 2004. Sensitization of multidrug resistant human osteosarcoma cells to Apo2 ligand/TRAIL-induced apoptosis by inhibition of the Akt/PKB kinase. Int. J. Oncol. 25, 1599–1608.

Chou, A.J., Gorlick, R., 2006. Chemotherapy resistance in osteosarcoma: current challenges and future directions. Expert Rev. Anticancer Ther. 6, 1075–1085.

Dobrowsky, R.T., Kamibayashi, C., Mumby, M.C., Hannun, Y.A., 1993. Ceramide activates heterotrimeric protein phosphatase 2A. J. Biol. Chem. 268, 15523–15530.

Gamble, J.R., Xia, P., Hahn, C.N., Drew, J.J., Drogemuller, C.J., Brown, D., Vadas, M.A., 2006. Phenoxodiol, an experimental anticancer drug, shows potent antiangiogenic properties in addition to its antitumour effects. Int. J. Cancer 118, 2412–2420.

Hait, N.C., Sarkar, S., Le Stunff, H., Mikami, A., Maceyka, M., Milstien, S., Spiegel, S., 2005. Role of sphingosine kinase 2 in cell migration toward epidermal growth factor. J. Biol. Chem. 280, 29462–29469.

Ji, C., Yang, B., Yang, Y.L., He, S.H., Miao, D.S., He, L., Bi, Z.G., 2010. Exogenous cell-permeable C6 ceramide sensitizes multiple cancer cell lines to Doxorubicin-induced apoptosis by promoting AMPK activation and mTORC1 inhibition. Oncogene 29, 6557–6568.

Jin, S., Pang, R.P., Shen, J.N., Huang, G., Wang, J., Zhou, J.G., 2007. Grifolin induces apoptosis via inhibition of PI3K/AKT signalling pathway in human osteosarcoma cells. Apoptosis 12, 1317–1326.

Kamsteeg, M., Rutherford, T., Sapi, E., Hanczaruk, B., Shahabi, S., Flick, M., Brown, D., Mor, G., 2003. Phenoxodiol – an isoflavone analog – induces apoptosis in chemoresistant ovarian cancer cells. Oncogene 22, 2611–2620.

Kandaswami, C., Lee, L.T., Lee, P.P., Hwang, J.J., Ke, F.C., Huang, Y.T., Lee, M.T., 2005. The antitumor activities of flavonoids. In Vivo 19, 895–909.

Kolesnick, R.N., Kronke, M., 1998. Regulation of ceramide production and apoptosis. Annu. Rev. Physiol. 60, 643–665.

Lamartiniere, C.A., Murrill, W.B., Manzolillo, P.A., Zhang, J.X., Barnes, S., Zhang, X., Wei, H., Brown, N.M., 1998. Genistein alters the ontogeny of mammary gland development and protects against chemically-induced mammary cancer in rats. Proc. Soc. Exp. Biol. Med. 217, 358–364.

Law, B., Rossie, S., 1995. The dimeric and catalytic subunit forms of protein phosphatase 2A from rat brain are stimulated by C2-ceramide. J. Biol. Chem. 270, 12808–12813.

Liu, B., Shi, Z.L., Feng, J., Tao, H.M., 2008. Celecoxib, a cyclooxygenase-2 inhibitor, induces apoptosis in human osteosarcoma cell line MG-63 via down-regulation of PI3K/Akt. Cell Biol. Int. 32, 494–501.

Liu, X., Ryland, L., Yang, J., Liao, A., Aliaga, C., Watts, R., Tan, S.F., Kaiser, J., Shanmugavelandy, S.S., Rogers, A., Loughran, K., Petersen, B., Yuen, J., Meng, F., Baab, K.T., Jarbadan, N.R., Broeg, K., Zhang, R., Liao, J., Sayers, T.J., Kester, M., Loughran Jr., T.P., 2010. Targeting of survivin by nanoliposomal ceramide induces complete remission in a rat model of NK-LGL leukemia. Blood 116, 4192–4201.

Maceyka, M., Payne, S.G., Milstien, S., Spiegel, S., 2002. Sphingosine kinase, sphingosine-1-phosphate, and apoptosis. Biochim. Biophys. Acta 1585, 193–201.

Merrill Jr., A.H., van Echten, G., Wang, E., Sandhoff, K., 1993. Fumonisin B1 inhibits sphingosine (sphinganine) N-acyltransferase and de novo sphingolipid biosynthesis in cultured neurons in situ. J. Biol. Chem. 268, 27299–27306.

Miltyk, W., Craciunescu, C.N., Fischer, L., Jeffcoat, R.A., Koch, M.A., Lopaczynski, W., Mahoney, C., Jeffcoat, R.A.,

Crowell, J., Paglieri, J., Zeisel, S.H., 2003. Lack of significant genotoxicity of purified soy isoflavones (genistein, daidzein, and glycitein) in 20 patients with prostate cancer. Am. J. Clin. Nutr. 77, 875–882.

Mor, G., Fu, H.H., Alvero, A.B., 2006. Phenoxodiol, a novel approach for the treatment of ovarian cancer. Curr. Opin. Investig. Drugs 7, 542–548.

Ogretmen, B., Hannun, Y.A., 2001. Updates on functions of ceramide in chemotherapy-induced cell death and in multidrug resistance. Drug Resist. Updat. 4, 368–377.

Okada, T., Kajimoto, T., Jahangeer, S., Nakamura, S., 2009. Sphingosine kinase/sphingosine 1-phosphate signalling in central nervous system. Cell. Signal. 21, 7–13.

Panaretakis, T., Laane, E., Pokrovskaja, K., Bjorklund, A.C., Moustakas, A., Zhivotovsky, B., Heyman, M., Shoshan, M.C., Grander, D., 2005. Doxorubicin requires the sequential activation of caspase-2, protein kinase Cdelta, and c-Jun NH2-terminal kinase to induce apoptosis. Mol. Biol. Cell 16, 3821–3831.

Park, J.H., Sihn, C.R., Lee, Y.S., Lee, S.J., Kim, S.H., 2011. Depletion of neuroguidin/CANu1 sensitizes human osteosarcoma U2OS cells to doxorubicin. BMB Rep. 44, 46–51.

Paugh, B.S., Paugh, S.W., Bryan, L., Kapitonov, D., Wilczynska, K.M., Gopalan, S.M., Rokita, H., Milstien, S., Spiegel, S., Kordula, T., 2008. EGF regulates plasminogen activator inhibitor-1 (PAI-1) by a pathway involving c-Src, PKCdelta, and sphingosine kinase 1 in glioblastoma cells. FASEB J. 22, 455–465.

Reynolds, C.P., Maurer, B.J., Kolesnick, R.N., 2004. Ceramide synthesis and metabolism as a target for cancer therapy. Cancer Lett. 206, 169–180.

Sabbadini, R.A., 2006. Targeting sphingosine-1-phosphate for cancer therapy. Br. J. Cancer 95, 1131–1135.

Sarkar, F.H., Li, Y., 2003. Soy isoflavones and cancer prevention. Cancer Invest. 21, 744–757.

Shida, D., Takabe, K., Kapitonov, D., Milstien, S., Spiegel, S., 2008. Targeting SphK1 as a new strategy against cancer. Curr. Drug Targets 9, 662–673.

Silasi, D.A., Alvero, A.B., Rutherford, T.J., Brown, D., Mor, G., 2009. Phenoxodiol: pharmacology and clinical experience in cancer monotherapy and in combination with chemotherapeutic drugs. Expert Opin. Pharmacother. 10, 1059–1067.

Tagaram, H.R., Divittore, N.A., Barth, B.M., Kaiser, J.M., Avella, D., Kimchi, E.T., Jiang, Y., Isom, H.C., Kester, M., Staveley-O'Carroll, K.F., 2011. Nanoliposomal ceramide prevents in vivo growth of hepatocellular carcinoma. Gut 60, 695–701.

Takimoto, C.H., Glover, K., Huang, X., Hayes, S.A., Gallot, L., Quinn, M., Jovanovic, B.D., Shapiro, A., Hernandez, L., Goetz, A., Llorens, V., Lieberman, R., Crowell, J.A., Poisson, B.A., Bergan, R.C., 2003. Phase I pharmacokinetic and pharmacodynamic analysis of unconjugated soy isoflavones administered to individuals with cancer. Cancer Epidemiol. Biomarkers Prev. 12, 1213–1221.

Tobiume, K., Matsuzawa, A., Takahashi, T., Nishitoh, H., Morita, K., Takeda, K., Minowa, O., Miyazono, K., Noda, T., Ichijo, H., 2001. ASK1 is required for sustained activations of JNK/p38 MAP kinases and apoptosis. EMBO Rep. 2, 222–228.

Vadas, M., Xia, P., McCaughan, G., Gamble, J., 2008. The role of sphingosine kinase 1 in cancer: oncogene or non-oncogene addiction? Biochim. Biophys. Acta 1781, 442–447.

van Lummel, M., van Blitterswijk, W.J., Vink, S.R., Veldman, R.J., van der Valk, M.A., Schipper, D., Dicheva, B.M., Eggermont, A.M., ten Hagen, T.L., Verheij, M., Koning, G.A., 2011. Enriching lipid nanovesicles with short-chain glucosylceramide improves doxorubicin delivery and efficacy in solid tumors. FASEB J. 25, 280–289.

Verheij, M., Bose, R., Lin, X.H., Yao, B., Jarvis, W.D., Grant, S., Birrer, M.J., Szabo, E., Zon, L.I., Kyriakis, J.M., Haimovitz-Friedman, A., Fuks, Z., Kolesnick, R.N., 1996. Requirement for ceramide-initiated SAPK/JNK signalling in stress-induced apoptosis. Nature 380, 75–79.

Wolff, R.A., Dobrowsky, R.T., Bielawska, A., Obeid, L.M., Hannun, Y.A., 1994. Role of ceramide-activated protein phosphatase in ceramide-mediated signal transduction. J. Biol. Chem. 269, 19605–19609.

Yu, S., Shen, G., Khor, T.O., Kim, J.H., Kong, A.N., 2008. Curcumin inhibits Akt/mammalian target of rapamycin signaling through protein phosphatase-dependent mechanism. Mol. Cancer Ther. 7, 2609–2620.

Zhu, Q.Y., Wang, Z., Ji, C., Cheng, L., Yang, Y.L., Ren, J., Jin, Y.H., Wang, Q.J., Gu, X.J., Bi, Z.G., Hu, G., Yang, Y., 2011. C6-ceramide synergistically potentiates the anti-tumor effects of histone deacetylase inhibitors via AKT dephosphorylation and alpha-tubulin hyperacetylation both in vitro and in vivo. Cell Death Dis. 2, e117.